Available online at www.sciencedirect.com
ScienceDirect
Bioorganic & Medicinal Chemistry 15 (2007) 5710–5718
Bioorganic & Medicinal Chemistry

A novel thrombin binding aptamer containing a G-LNA residue

Ada Virno,[a] Antonio Randazzo,[a] Concetta Giancola,[b] Mariarosaria Bucci,[c] Giuseppe Cirino[c] and Luciano Mayol[a,*]

[a]*Dipartimento di Chimica delle Sostanze Naturali, Università degli Studi di Napoli "Federico II", via D. Montesano 49, I-80131 Napoli, Italy*
[b]*Dipartimento di Chimica, Università degli Studi di Napoli "Federico II", via Cintia, I-80126, Napoli, Italy*
[c]*Dipartimento di Farmacologia Sperimentale, Università degli Studi di Napoli "Federico II", via D. Montesano 49, I-80131 Napoli, Italy*

Received 5 April 2007; revised 28 May 2007; accepted 5 June 2007
Available online 8 June 2007

Abstract—In this work, we report the solution structure, thermodynamic studies, and the pharmacological properties of a new modified thrombin binding aptamer (TBA) containing a G-LNA residue, namely d(5′-GGTTGGTGTGGTTGg-3′), where upper case and lower case letters represent DNA and LNA residues, respectively. NMR and CD spectroscopy, as well as molecular dynamics and mechanic calculations, has been used to characterize the three-dimensional structure. The modified oligonucleotide is characterized by a chair-like structure consisting of two G-tetrads connected by three edge-wise TT, TGT, and TT loops. d(5′-GGTTGGTGTGGTTGg-3′) is characterized by the same folding of TBA, being two strands parallel to each other and two strands oriented in opposite manner. This led to a *syn–anti–syn–anti* and *anti–syn–anti–syn* arrangements of the Gs in the two tetrads. d(5′-GGTTGGTGTGGTTGg-3′) possesses an anticoagulant activity, even if decreased with respect to the TBA.

1. Introduction

The prospect of preparing therapeutically active analogues of natural nucleic acids has stimulated much interest to improve their characteristics, such as hybridization affinity, stability toward cellular nucleases, and the ability to penetrate the cell membrane.[1]

In the last two decades a variety of modified oligonucleotides have been synthesized and they are used now in biophysical and biochemical studies.[2]

In 1998, for example, the first oligonucleotides containing one or more 2′-*O*,4′-*C* methylene-linked bicyclic ribonucleosides (LNA, Locked Nucleic Acid) were prepared by the groups of Wengel[3,4] and Imanishi.[5] They also described the hybridization affinity of LNAs toward complementary nucleic acids. In LNA, the furanose conformation is chemically locked in a C3′-endo (N-type) conformation by the introduction of a 2′-*O*, 4′-*C* methylene linkage. LNAs have shown thermal affinities when hybridized with either DNA (ΔT_m = 1–8 °C per modification), RNA (ΔT_m = 2–10 °C per modification) or LNA (ΔT_m 5 °C per modification).[6–9]

The hybridization properties suggest that LNAs could be used as powerful agents for fine tuning drugs with a very specific target potential, thus providing a new class of therapeutics.[7] Actually, LNAs represent very versatile tools for the control of gene expression, the treatment of various human diseases, and diagnostic assays. In fact, chimeric 2′-*O*-methyl/LNA oligoribonucleotides were found to inhibit RNA-protein interactions important for HIV replication by sterically blocking the *trans*-activation responsive region TAR.[10] Furthermore, incorporation of LNA monomers into the binding arms of the '10-23' DNAzyme, yielding an LNAzyme, markedly increases cleavage properties toward the target RNA.[11]

Furthermore, a paper of some of us, in which we reported the NMR solution structure of a parallel LNA quadruplex,[12] underscored further the wide range of applicability of LNAs. Nevertheless, very little is known about the effects of the incorporation of LNA residues in antiparallel quadruplex structures.[13] DNA quadruplex

Keywords: DNA; LNA; Quadruplex; TBA; NMR; Anticoagulant activity.
* Corresponding author. Tel.: +39 081 678508; fax: +39 081 678552; e-mail: mayoll@unina.it

0968-0896/$ - see front matter © 2007 Elsevier Ltd. All rights reserved.
doi:10.1016/j.bmc.2007.06.008

structures have been found in a number of important DNA regions, such as those present at the ends of telomeres,[14] in the promoter region of c-myc and other oncogenes, in upstream of the insulin gene,[15] and in the structures of some aptamers.

Aptamers[16] are nucleic acid macromolecules that bind to molecular targets, including proteins, with high affinity and specificity. Aptamers are typically from 15 to 40 nucleotides in length and can be composed of DNA and RNA. Base composition defines aptamer secondary structure, consisting primarily of helical arms and single-stranded loops. Stable tertiary structure, resulting from combinations of these secondary structures, allows aptamers to bind to targets via van der Waals, hydrogen bonding, and electrostatic interaction.

The aptamer drug TBA (Thrombin Binding Aptamer), also named ARC183 (Archemix Corp.), is a consensus DNA 15-mer, namely 5-′GGTTGGTGTGGTTG G-3′,[17–19] discovered with this technique. The three-dimensional solution structure of TBA was solved using NMR and X-ray techniques.[20,21] TBA is characterized by a chair-like quadruplex structure consisting of two G-tetrads connected by two TT loops and a single TGT loop. The aptamer is a thrombin inhibitor in development for use as an anticoagulant during coronary artery bypass graft procedures. Currently, the only approved anticoagulant for coronary artery bypass graft is heparin. TBA exhibits a K_D of 2 nM for thrombin, 50 nM for prothrombin, and binding to other serum proteins or proteolytic enzymes is essentially undetectable.[16] As suggested by others,[22] TBA binds at the anion exosite I of thrombin in a conformation little changed from that of the unbound species. TBA is a strong anticoagulant in vitro, and inhibits thrombin-catalyzed activation of fibrinogen and thrombin induced platelet aggregation. TBA has key advantages in that it avoids heparin use and the risk of associated thrombocytopenia, is a specific inhibitor with rapid onset, is effective at inhibiting clot-bound thrombin, and has a short in vivo half-life of approximately 2 min which allows for rapid reversal of its effects and the avoidance of dose-adjusting complications of heparin and protamine. Neither significant toxicities nor excessive bleeding intraoperatively has been observed.

In order to improve the properties of TBA, a number of researches[22–25] have been devoted to its structure–activity relationship to *post*-SELEX modifications. For example, He et al.[24] synthesized numerous TBA analogues containing modified guanosine carrying several substituents at 8 position or at the exocyclic amino group. In a different paper,[25] the same authors reported the synthesis and the thrombin inhibiting properties of several TBA based oligonucleotides containing neutral formacetal linkages.

In this frame, we have undertaken a study whose aim is to use a biologically driven approach in order to improve the knowledge of the interactions between thrombin and TBA, that are critical for the biological activity. Furthermore, this study wants to demonstrate that LNA residues can be incorporated in an antiparallel quadruplex forming oligonucleotide.

Thus, here we report the study of four new TBA based oligonucleotides containing LNA residues, namely 5′-ggttggtgtggttgg-3 (**1**), 5′-ggTTggTGTggTTgg-3′ (**2**), 5′-gGTTGGTGTGGTTGG-3′ (**3**), and 5′-GGTTGG TGTGGTTGg-3′ (**4**), where upper case and lower case letters represent DNA and LNA residues, respectively. Moreover, the chemical-physical properties and the three-dimensional characterization, based on NMR and CD spectroscopy, associated with molecular mechanics and dynamics calculations, of **4** are also reported.

2. Results and discussion

The synthesis of the oligoribonucleotides 5′-ggttggtg tggttgg-3′ (**1**), 5′-ggTTggTGTggTTgg-3′ (**2**), 5′-gGTT GGTGTGGTTGG-3′ (**3**) and 5′-GGTTGGTGTGGTT Gg-3′ (**4**) was performed by standard methods and the incorporation of modified residues was performed using G-LNA (g) or T-LNA (t) phosphoramidites. The NMR samples of **1**–**4** were prepared at a concentration of 2.0 mM (0.6 ml, 90% H_2O/10% D_2O) in 10 mM KH_2PO_4 buffer containing 70 mM KCl, 0.2 mM EDTA (pH 7.0). The samples were heated for 10 min at 80 °C and slowly cooled down to room temperature, then their ^{1}H NMR spectra were recorded by using pulsed-field gradient WATERGATE[27] for H_2O suppression. The lack of imino signals in the 1D ^{1}H NMR spectrum of the oligomer containing all LNA residues (**1**) indicates that, in the conditions used here, it is unstructured, most probably due to the decreased flexibility of the molecule now containing LNA residues. On the other hand, **2** and **3** give NMR spectra characteristic of mixtures of different structures. As far as **1**–**3** are concerned, neither varying buffer solutions (using alternatively potassium and sodium buffers and changing the concentrations of both KCl and NaCl), nor varying the temperature could improve the quality of their spectra. The oligonucleotides 5′-GGTTGGTGTGGTTGg-3′ (**4**), instead, turned out to be the only analyzed oligonucleotide capable to form a single well-defined hydrogen-bonded structure in solution. In fact, with the exclusion of some weak resonances due to very minor conformations also present in solution (whose relative intensities turned out to be insensitive to temperature changes), only fifteen signals attributable to nine guanine H8 and six thymine H6 protons were clearly observable in the aromatic region (Fig. 1).

A combination of the analysis of 2D NOESY (700 MHz, $T = 25$ °C), TOCSY spectra (700 MHz, $T = 25$ °C), and ^{31}P NMR spectroscopy (202 MHz, $T = 25$ °C) allowed us to get the almost complete assignment (Table 1) of both exchangeable and nonexchangeable protons, and phosphorus resonances of **4**. Particularly, the one-dimensional proton decoupled phosphorus spectrum displays 14 signals (see Supplementary material). After assigning the ^{1}H resonances within each deoxyribose by a 2D TOCSY experiment,

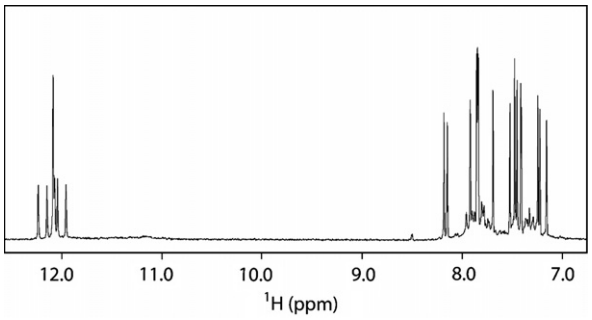

Figure 1. Expanded region of the proton NMR spectrum of **4** (700 MHz, $T = 25$ °C).

the 2D proton-detected heteronuclear ^{1}H-^{31}P COSY (see Supplementary material) allowed us to assign the entire backbone correlating each phosphorus resonance to the respective H3′ proton on the 5′-side and H5′/H5″ protons on the 3′-side. Further, NOEs between base protons and H1′, H2′ and H2″ protons allowed us to assign all aromatic protons to the pertinent base.

It is interesting to note that the intensities of NOESY (700 MHz, $T = 25$ °C, mixing time 100 ms) crosspeaks between the H8 proton bases and sugar H1′ resonances indicate that four (G1, G5, G10, G14) out of nine Gs of **4** adopt a *syn* glycosidic conformation (Fig. 2), where the H8 resonances of *syn* G residues are upfield shifted with respect to those of the *anti* ones.[20,26,27]

Then, four *anti*-Gs (G2, G6, G11, and G15) have classical H8/H2′–H2″ sequential connectivities to 5′ neighboring *syn*-Gs (G1, G5, G10, and G14, respectively) (Fig. 3), indicating that the subunits G1–G2, G5–G6, G10–G11, and G14–G15 are involved in the formation of a four-stranded helical structure (underlined residues adopt a *syn* glycosidic conformation). Moreover, the entire pattern of NOEs observed for all cited Gs indicates that the backbone conformations of these tracts resemble those of the unmodified TBA possessing a right-handed helix structure (Fig. 3).

The alternation of *syn* and *anti* G residues within each strand suggests that, as TBA, **4** folds into a monomolecular foldback quadruplex, characterized by two G tetrads. Further, a number of unusual NOE connectivities were observed between *syn*-Gs and Ts, indicating that 5′-TG-3′ and 5′-GT-3′ tracts do not adopt a helical winding, thus suggesting that, most probably, the TT and TGT tracts form loops. Thus, **4** is characterized by two G tetrads formed by the residues G1, G6, G10, G15 and G2, G5, G11, G14, respectively, where the underlined residues possess a *syn* glycosidic conformation. Interestingly the two tetrads assume a *syn–anti–syn–anti* and *anti–syn–anti–syn* arrangement of the bases. Then, the facts that TGT loop possesses some NOEs with G imino protons of one tetrad and that the two TT loops are characterized by NOEs with G imino protons of the other tetrad indicate that no loop assumes a dog-eared conformation. All this means that **4** folds into a chair-like quadruplex structure characterized by the same folding observed for TBA, possessing four strands, two by two parallel to each.

In order to calculate the three-dimensional structure of **4** at atomic level, an estimation of proton–proton distances has been done analyzing the cross-peak intensities

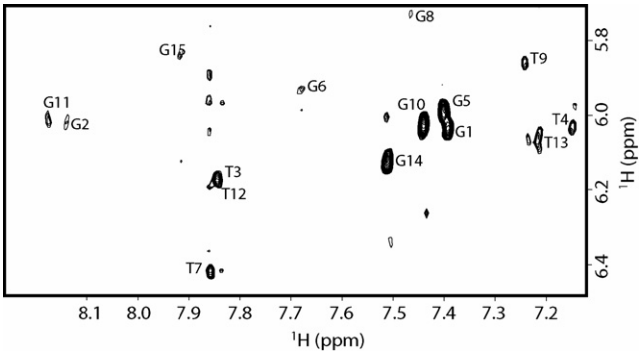

Figure 2. Expanded region of the NOESY spectrum of **4** (700 MHz, $T = 25$ °C, mt = 200 ms) correlating G–H8/H1′ protons.

Table 1. Proton (700 MHz) and phosphorus (202 MHz) chemical shifts of **4** in 10 mM KH_2PO_4, 70 mM KCl, 0.2 EDTA (pH 7.0, $T = 25$ °C)

Base (5′–3′)	H8/H6	H1′	H2′	H2″	H3′	H4′	H5′/H5″[a]	H6′/H6″[a]	H2/Me	^{31}P
G1	7.41	6.04	2.94	2.94	4.98	4.37	3.98/4.05			
G2	8.14	6.01	2.98	2.35	5.13	4.39	4.40			−2.09
T3	7.84	6.18	2.17	2.54	4.89	4.28	4.29/4.27		1.96	−0.18
T4	7.15	6.04	2.06	2.61	4.88	4.23	4.38/4.30		1.03	−2.24
G5	7.40	5.99	3.37	2.86	4.85	4.42	4.27			−1.03
G6	7.68	5.94	2.74	2.57	5.10	4.41	4.23/4.41			−2.01
T7	7.85	6.42	2.47	2.59	4.84	4.42	4.23/3.91		1.96	−1.10
G8	7.47	5.72	2.03	2.34	4.74	4.07	4.03			−1.57
T9	7.24	5.86	1.95	2.36	4.61	3.01	3.66/3.55		1.65	−1.81
G10	7.45	6.03	3.66	2.94	4.89	4.26	4.10/4.12			−2.13
G11	8.17	6.00	2.95	2.35	5.13	4.39	4.20/4.18			−1.10
T12	7.84	6.18	2.17	2.54	4.89	4.28	4.29/4.27		1.96	−0.24
T13	7.22	6.07	2.12	2.64	4.90	4.27	4.16/3.90		0.96	−0.95
G14	7.51	6.13	3.86	3.01	4.97	4.37	4.10/4.34			−1.46
g15	4.91	5.81	4.86		4.49		4.36	4.11/3.92		−1.90

[a] No stereospecific assignment has been done.

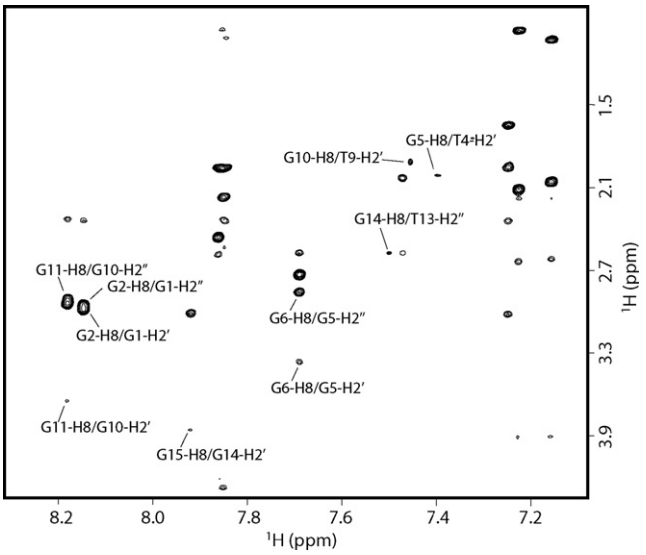

Figure 3. Expanded region of NOESY spectrum of **4** (700 MHz, $T = 25$ °C, mt = 100 ms) correlating G–H8/H2′–H2″ protons. Classical G–H8/H2′–H2″ NOEs correlations for the four-stranded part of the complex are reported.

in 2D NOESY experiments acquired at 700 MHz, both at $T = 25$ °C and $T = 5$ °C (mixing time 100 ms for the experiment acquired in D_2O and 200 ms for the experiments acquired in H_2O). No spin diffusion phenomenon has been observed using both 100 ms and 200 ms mixing times. Pseudo-atoms were introduced where needed. Distances (138) were used for the calculations and, as suggested by the presence of eight G imino protons in the 1D ^{1}H NMR spectrum, 32 supplementary distance restraints (HN1–O6, N1–O6, HN2–N7, N2–N7) for 16 hydrogen bonds corresponding to the two G-quartets were incorporated during the computations (Table 2). Further, in agreement with NMR data, glycosidic torsion angles for four out of eight guanines involved in the formation of the two G-tetrads were fixed in the *anti*-domain (−160°/−70°), whereas the χ angle was kept in a range of 10°/100° (*syn*-conformation) for the remaining four G residues.

Therefore, three-dimensional structures which satisfy NOEs were constructed by simulated annealing (SA)

Table 2. Experimental constraints and structure statistics of the best 20 structures of **4**

Experimental constraints	
Total NOEs	138
NOEs from nonexchangeable protons	117
NOEs from exchangeable protons	21
Hydrogen bonds constraints	36
Dihedral angle constraints	8
CVFF energy (kcal mol^{-1}) of the minimized structures	
Total	−4282.250 ± 2.396
Nonbond	143.685 ± 3.112
Restraint	18.979 ± 1.085
RMS deviations from the mean structure (Å)	
All backbone heavy atoms	0.80 ± 0.24
All heavy atoms	0.88 ± 0.29

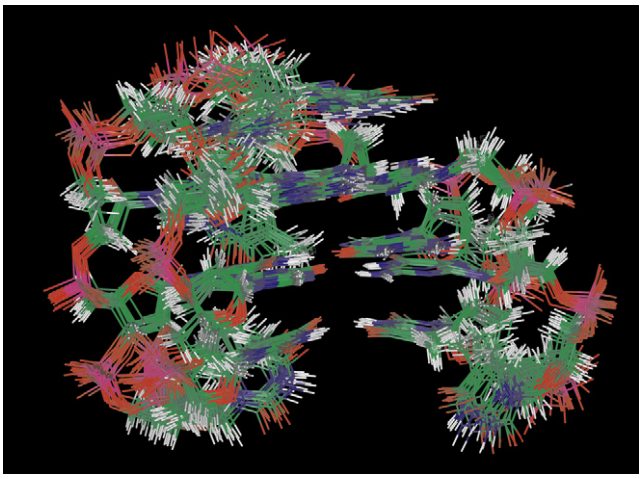

Figure 4. Side view representation of the superimposed 20 structures of **4**. Backbones and bases are depicted in colored 'stick' (carbons, green; nitrogens, blue; oxygens, red; hydrogens, white).

calculations. An initial structure of the oligonucleotide was constructed possessing a random conformation and minimized, in order to eliminate any possible source of initial bias in the folding pathway. Restrained simulations were carried out for 500 ps using the CVFF force field as implemented in Discover software (Accelrys, San Diego, USA). The restrained SA calculations started at 1000 K, and, thereafter, the temperature was decreased stepwise down to 273 K. The aim of this step was to energy-minimize and refine the structures obtained by using the steepest descent followed by the quasi-Newton–Raphson (VA09A) algorithms. A total of 20 structures was generated. Average RMSD values of 0.80 ± 0.24 Å and 0.88 ± 0.29 Å for the backbone and all heavy atoms, respectively, were obtained from the superimposition of all the 20 structures (Fig. 4). These data, along with the lack of significant violations of the experimental restraints, suggest that the obtained structures are representative of the structure actually adopted in solution by **4**.

As expected, **4** shows a right-handed helical backbone geometry and three edge-wise connecting TT, TGT, and TT loops. As the unmodified TBA, **4** involves two stacked G-tetrads, with the same guanine *syn*/*anti* distribution around the GGGG tetrads, being characterized by the usual *syn–anti–syn–anti* and *anti–syn–anti–syn* arrangement of the two tetrads, respectively, and in the relative strand orientations, with two strands parallel to each other and two strands oriented in opposite manner.

A direct comparison of the most representative structure of **4** (the one with lowest energy after minimization), and the already reported NMR structure of the unmodified TBA (PDB code: 148D) has been accomplished by analyzing the helix parameters by CURVES[28,29] (Tables 3 and 4).

These data clearly suggest that the overall structure adopted by **4** is similar to that of TBA. The base stacking of the two quadruplexes is quite similar, being the

Table 3. Rise, Tilt, Roll, and Twist of TBA and of the best-minimized structure of **4**

TBA	Rise	Tilt	Roll	Twist	**4**
G1/G2	3.44	−10.60	−179.75	50.93	
	−3.27	−13.21	−171.63	53.01	G1/G2
G5/G6	2.67	6.22	−161.77	48.90	
	−2.78	5.99	−177.02	53.01	G5/G6
G10/G11	2.80	10.45	−178.83	48.50	
	−2.69	19.14	162.67	53.27	G10/G11
G14/G15	4.67	−17.19	−177.35	55.65	
	−3.79	−4.11	−174.67	51.53	G14/G15

Table 4. Shear, Stretch, Stagger, Buckle, Propeller, Opening of **TBA** and of the best-minimized structure of **4**

TBA	Shear	Stretch	Stagger	**4**
G1/G6	−6.15	1.72	−0.88	
	−6.39	0.59	−0.47	G1/G6
G1/G10	4.82	2.32	−2.69	
	6.59	2.66	−1.05	G1/G10
G1/G15	−6.02	1.87	−0.59	
	−4.47	2.83	−0.18	G1/G15
G2/G5	6.42	2.77	−0.11	
	6.50	3.80	0.03	G2/G5
G2/G11	−6.04	1.75	−2.05	
	−5.88	4.29	−0.47	G2/G11
G2/G14	5.41	2.07	−1.82	
	5.95	5.06	−0.69	G2/G14
TBA	Buckle	Propeller	Opening	**4**
G1/G6	11.32	176.45	−89.48	
	9.96	−173.55	−90.27	G1/G6
G1/G10	3.47	−176.25	−0.95	
	−13.52	179.48	−0.57	G1/G10
G1/G15	−5.12	−162.35	86.32	
	4.42	−156.38	88.74	G1/G15
G2/G5	−5.50	157.97	−91.51	
	−9.24	175.09	−91.16	G2/G5
G2/G11	24.52	−177.68	−3.39	
	18.83	−171.56	−1.20	G2/G11
G2/G14	−5.12	−162.35	86.32	
	−4.68	−170.08	86.37	G2/G14

five-membered rings of the top guanines overlapped to the five-membered rings of the underneath guanine bases.

As for the sugar puckering, the two molecules possess almost the same sugar ring conformations except for the G1, G10, G11, and G15 that in **4** adopt a C4′-*exo*, C3′-*endo*, C3′-*endo*, and C3′-*endo* conformations, respectively.

It is interesting to note that one structural difference relies on the orientation of T7, that folds back into the groove formed by the strands G5–G6 and G10–G11 (Fig. 5).

In order to determine the effects of the introduction of a modified residue on the CD profile and the thermal stability of the resulting quadruplex structure, CD spectra and CD melting and annealing experiments were acquired for **4** (Fig. 6A) and its natural counterpart (see Supplementary material). In particular, the CD spectra of **4** and TBA, performed at 20 °C, are almost superimposable, both exhibiting two positive bands at 248 and 294 nm and a negative one at 267 nm, typical of antiparallel quadruplex structures,[30–32] containing residues in *syn*-glycosidic conformations.

As for melting and annealing CD experiments, taking into account that the rates of quadruplex formation/dissociation are very slow, we collected the data at 10°C/h. No significant hysteresis emerged for both **4** (Fig. 6B) and TBA (see Supplementary material) comparing annealing and melting curves thereby indicating that, at the scan rate used, both systems were at equilibrium. Therefore, the melting temperatures of 46 and 52 °C could be measured for **4** and TBA, respectively. The melting curves were analyzed using van't Hoff analysis (Fig. 7) and thermodynamic parameters are shown in Table 5. The data, compared with those of unmodified TBA, indicate that the introduction of a LNA residue destabilizes the TBA structure. $\Delta H°$ values for the two

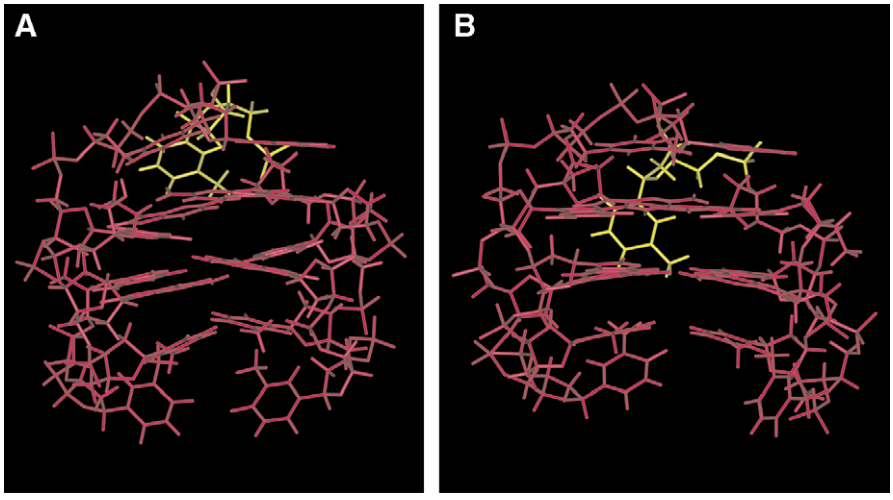

Figure 5. Side view of TBA (A) and 4 (B). Backbones and bases are depicted in colored 'stick' (magenta). The different orientation of T7 (in yellow) is highlighted.

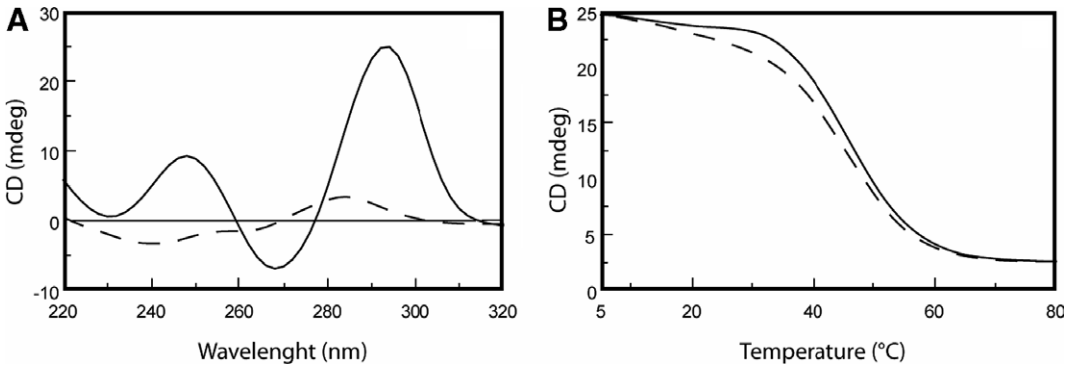

Figure 6. (A) CD spectra of **4** at 20 °C (continuous lines) and 90 °C (dashed lines). (B) Melting (continuous lines) and annealing (dashed lines) CD experiments of **4**.

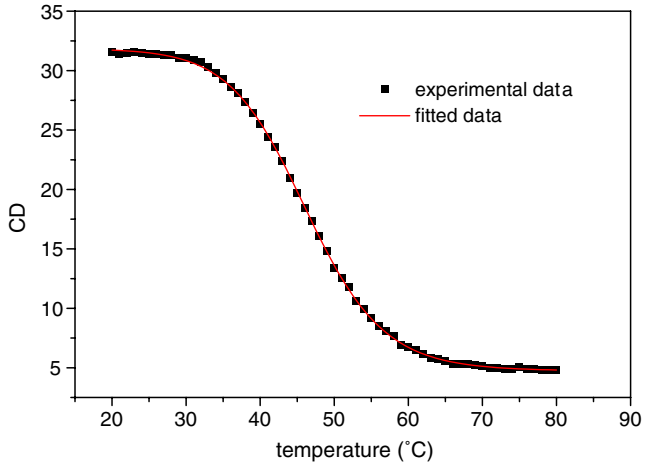

Figure 7. Fitting of CD melting data of **4** according to the van't Hoff analysis.

Table 5. Thermodynamic parameters for the unfolding of **4** and TBA

	T_m °C (±1)	$\Delta H°$ kJ mol^{-1} (±20)	$\Delta S°$ kJ mol^{-1} K^{-1} (±0.05)	$\Delta G°$(298 K) kJ mol^{-1} (±1)
4	46	163	0.51	10
TBA	52	160	0.49	13

aptamers are similar and correspond to a value of $\Delta H°$ of dissociation of about 80 kJ mol^{-1} for G-tetrad, in accord with previously reported values.[33,34] The enthalpic data are in line with NMR data that show for the two quadruplexes a very similar geometry of the G-tetrads. Since $\Delta H°$ values are comparable and the T_m of **4** is lower, the lower thermodynamic stability is entropically controlled. In fact, the presence of a conformationally locked nucleotide increases the local organization of the phosphodiester backbone lowering the entropic content in the quadruplex with a consequence of a major gain in entropy in the dissociation process.

The biological activity of **1**–**4** has been tested with a prothrombin time (PT) assay.

The PT assay (or INR or Quick time) is a routinely diagnostic assay that evaluates in vitro the activation of extrinsic pathway of the coagulation cascade. This ultimately measures the conversion of fibrinogen in fibrin by thrombin with formation of a solid gel clot. In healthy subject the PT is about 12 s and is highly reproducible. Any compound that prolongs this value could be considered a potential anticoagulant.

PT assays on all four samples were performed on human plasma in strict comparison with TBA. In order to eliminate the variation caused by the measurements performed on different days, the samples of **1**, **2**, **3**, **4**, and TBA were prepared at the same time and folded together by heating the samples for 10 min at 80 °C and slowly cooling them down at room temperature. The assays have been conducted after 1 week from the preparation procedure. Samples **1**–**3** did not show any prolonged PT, and therefore any significant activity. On the other hand, **4** displayed a prolonged PT. However, as shown in Figure 8, the activity of TBA (at the concentration of 20 μM) on PT measurement turned to be more marked when compared with **4** in the same time frame. It is interesting to note that only the magnitude of the activity of **4** was reduced when compared to TBA since the onset as well as the endurance of the activity were almost comparable. The same assay performed by using a minor concentration of the compounds (2 μM) resulted in a loss of anticoagulant activity after 5 min of incubation for **4** while TBA preserved its anticoagulant activity up to 15 min (data not shown). The biological data reported here imply that the modifications of the structure adopted by **4** affect the biological activity, and therefore its interaction with the thrombin. Looking to the overall folding of the modified aptamer, it was not expected such reduction in the biological activity. However, it is interesting to note that TBA inhibits the thrombin activity when interacting with its fibrinogen exosite.[35] In particular, it has been proposed TBA could associate with thrombin in two different ways: through the T7-G8-T9 loop (as suggested by X-ray data) or through the T3 and T12 residues (as suggested by NMR models).[35] It is already highlighted the role of the conformation of the loops in another modified TBA.[36] However, the very little difference in the orientation of T7 does not seem to fully justify such a reduction of biological activity. Therefore, the reduced activity of **4** might suggest that the mode of

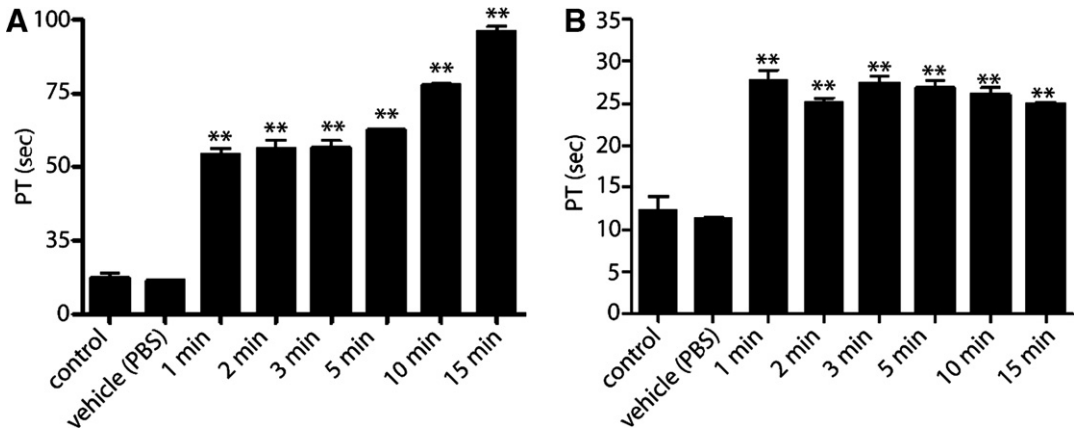

Figure 8. Prothrombin time assessed by using human plasma. On the *x*-axis the minutes of incubation are reported, while PT in seconds is reported on *y*-axis. (A) Refers to TBA, while (B) to **4**.

action of TBA actually requires a more wide recognition process that involves even locally a single residue.

The structures reported here are, to the best of our knowledge, the first example of an antiparallel quadruplex structure containing an LNA residue. These results, particularly when viewed in the context of other recent findings about locked nucleic acids, serve to underscore further the polymorphic nature of LNAs. Furthermore, the many advantageous characteristics of LNA usage, demonstrate that LNAs might amplify the range of applicability of synthetic oligonucleotides as aptamers. Moreover, the data reported here might give a further insight into the understanding of the variables involved in the mode of action of TBA and thus it is possible to take advantage of these findings to design new thrombin binding aptamers.

3. Materials and methods

The oligonucleotides 5′-ggttggtgtggttgg-3′ (**1**), 5′-ggTTg gTGTggTTgg-3′ (**2**), 5′-gGTTGGTGTGGTTGG-3′ (**3**), and 5′-GGTTGGTGTGGTTGg-3′ (**4**), and the natural counterpart 5′-GGTTGGTGTGGTTGG-3′ (TBA) were synthesized on a Millipore Cyclon Plus DNA synthesizer, using solid phase β-cyanoethyl phosphoramidite chemistry at 15 μmol scale. The syntheses of the oligonucleotides were performed by standard methods and using G- and T-LNA phosphoramidites for the modified residue. The oligomers were detached from the support and deprotected by treatment with concd aq ammonia at 55 °C for 12 h. The combined filtrates and washings were concentrated under reduced pressure, redissolved in H_2O and analyzed and purified by HPLC on a Nucleogel SAX column (Macherey-Nagel, 1000-8/46); using buffer A: 20 mM KH_2PO_4 aq solution, pH 7.0, containing 20% (v/v) CH_3CN; buffer B: 1 M KCl, 20 mM KH_2PO_4 aqueous solution, pH 7.0, containing 20% (v/v) CH_3CN; a linear gradient from 0 to 100 % B in 30 min and flow rate 1 mL/min were used. The oligomers were collected and successively desalted by Sep-Pak cartridges (C18). The isolated oligomers were more than 99% pure (NMR).

3.1. Nuclear magnetic resonances

NMR samples were prepared at a concentration of approximately 2 mM, in 0.6 ml (H_2O/D_2O, 9:1) buffer solution having 10 mM KH_2PO_4, 70 mM KCl, 0.2 mM EDTA, pH 7.0. For D_2O experiments, the H_2O was replaced with D_2O by drying down the sample, lyophilization, and redissolution in D_2O alone. NMR spectra were recorded with Varian ^{Unity}INOVA 500 MHz and 700 MHz spectrometers. ^1H chemical shifts were referenced relative to external sodium 2,2-dimethyl-2-silapentane-5-sulfonate (DSS), whereas ^{31}P chemical shifts were referenced to external phosphoric acid (H_3PO_4 85% v/v). 1D proton spectra of samples in H_2O were recorded using pulsed-field gradient WATERGATE[37] for H_2O suppression. A proton-detected ^1H–^{31}P heteronuclear COSY was recorded in D_2O in the hypercomplex mode with 2048 t_2 points and 96 t_1 increments, and a spectral width of 500 Hz along the ^{31}P dimension. Phase sensitive NOESY spectra[38] were recorded with mixing times of 100 and 200 ms (T = 25 and 5 °C). Pulsed-field gradient WATERGATE was used for NOESY spectra in H_2O. TOCSY spectra[39] with mixing times of 100 ms were recorded with D_2O solutions.

All experiments were recorded using STATES-TPPI[40] procedure for quadrature detection. In all 2D experiments the time domain data consisted of 2048 complex points in t_2 and 400-512 fids in t_1 dimension. The relaxation delay was kept at 3 s for NOESY experiments used in the structure determination. A relaxation delay of 1.2 s was used for all other experiments. The NMR data were processed on a SGI Octane workstation using FELIX 98 software (Accelrys, San Diego, CA).

3.2. Structural calculations

Structure calculations of **4** have been performed as follow: cross peak volume integrations were performed with the program FELIX 98, using the NOESY experiment collected at mixing time of 100 ms. The NOE volumes were then converted to distance restraints after they were calibrated using known fixed distances of H2′/H2″ of G5, G8, G10, T12, and G14. Then a NOE

restraint file was generated with three distance classifications as follows: strong NOEs (1.8 Å $\leqslant r_{ij} \leqslant$ 3.0 Å, where r_{ij} is the interproton distance between protons i,j), medium NOEs (2.5 Å $\leqslant r_{ij} \leqslant$ 4.0 Å), and weak NOEs (3.5 Å $\leqslant r_{ij} \leqslant$ 5.5 Å). A total of 138 NOE-derived distance restraints were used.

Hydrogen bonds constraints were used: upper and lower distance limits of 2.0 Å and 1.7 Å for hydrogen-acceptor distance, and 3.0 Å and 2.7 Å for donor–acceptor distance, respectively. These constraints for H-bonds did not lead to an increase in residual constraints violation. No backbone torsion angles were used. According to NMR data, glycosidic torsion angles were kept in a range of −160°/−70° for the G *anti*, whereas a range of 10°/100° was used for the G *syn*.

The calculations have been performed using a distance dependent macroscopic dielectric constant of 4*r and an infinite cut-off for nonbonded interactions to partially compensate for the lack of the solvent.[41] Thus the three-dimensional structures which satisfy NOE and dihedral angle constraints were constructed by simulated annealing calculations. An initial structure of the oligonucleotide was built using a completely random array of atoms. Using the steepest descent followed by quasi-Newton–Raphson method (VA09A) the conformational energy was minimized. Restrained simulations were carried out for 500 ps using the CVFF force field as implemented in Discover software (Accelrys, San Diego, USA). The simulation started at 1000 K, and then the temperature was decreased stepwise until 273 K. The final step was again to energy-minimize to refine the structures obtained, using successively the steepest descent and the quasi-Newton–Raphson (VA09A) algorithms. Both dynamic and mechanic calculations were carried out by using 1 (kcal/mol)/Å^2 flatwell distance restraints. Twenty structures were generated. RMSD values of 0.80 ± 0.24 Å and 0.88 ± 0.29 Å for the backbone and heavy atoms, respectively, were calculated for all the 20 structures.

Illustrations of structures were generated using the INSIGHT II program, version 2005 (Accelrys, San Diego, USA). All the calculations were performed on a PC running Linux WS 4.0.

3.3. Circular dichroism

CD samples of **4** and TBA were prepared at a concentration of 1×10^{-4} M, by using the buffer solution used for NMR experiments: 10 mM KH_2PO_4, 70 mM KCl, 0.2 mM EDTA, pH 7.0. CD spectra and CD melting curves were registered on a Jasco 715 circular dichroism spectrophotometer in a 0.1 cm pathlength cuvette. For the CD spectra, the wavelength was varied from 220 to 320 nm at 100 nm min^{-1}, and the spectra recorded with a response of 16 s, at 2.0 nm bandwidth and normalized by subtraction of the background scan with buffer. The temperature was kept constant at 20 °C with a thermoelectrically controlled cell holder (Jasco PTC-348). CD melting curves were registered as a function of temperature from 20 to 90 °C at 294 nm with a scan rate of 10 °C h^{-1} for both quadruplexes. The CD melting curves of TBA and modified aptamer showed sigmoidal profiles and were modeled by a two-state transition, using a theoretical equation for an intramolecular association, according to the van't Hoff analysis.[42] The T_m and $\Delta H°$ values provide the best fit of the experimental melting data. The reported errors for thermodynamic parameters are the standard deviations of the mean from the multiple determinations. The $\Delta S°$ values were calculated by equation $\Delta S° = \Delta H°/T_m$ and free energy change values by the equation $\Delta G°(T) = \Delta H° - T\Delta S°$.

3.4. Prothrombin time (PT) assay

Human plasma samples were collected by venipuncture, in presence of 0.1 volumes 3.8% sodium citrate and fractionated by centrifugation at 2000*g* for 5 min. PT times were measured by using Koagulab MJ Coagulation System with a specific kit RecombiPlas Tin HemosIL (Inst. Labs, Lexinton, USA). Briefly, this method relies on the high sensitivity thromboplastin reagent based on recombinant human tissue factor. The addition of recombiplastin to the plasma in presence of calcium ions initiates the activation of extrinsic pathway. This results ultimately in the conversion of fibrinogen to fibrin, with a formation of solid gel. The procedure was performed according to the manufacturer's instructions. TBA, **1**, **2**, **3**, and **4** or vehicle (PBS) were added at different time points in volume of 2 μl at final concentration of 20 μM. Data are expressed as means ± SEM and are representative of at least three different measurements.

Acknowledgments

This work was supported by Italian M.U.R.S.T. (P.R.I.N. 2005 and 2006) and Regione Campania (L.41, L.5). The authors are grateful to Centro di Servizio Interdipartimentale di Analisi Strumentale, C.S.I.A.S., for supplying NMR facilities.

Supplementary data

Supplementary data associated with this article can be found, in the online version, at doi:10.1016/j.bmc.2007.06.008.

References and notes

1. Hanss, B.; Leal-Pinto, E.; Bruggeman, L. A.; Copeland, T. D.; Klotman, P. E. *Proc. Natl. Acad. Sci.* **1998**, *95*, 1921.
2. Verma, S.; Eckstein, F. *Annu. Rev. Biochem.* **1998**, *67*, 99.
3. Koshkin, A. A.; Rajwanshi, V. K.; Wengel, J. *Tetrahedron Lett.* **1998**, *39*, 4381.
4. Wengel, J. *Acc. Chem. Res.* **1998**, *32*, 301.
5. Obika, S.; Nanbu, D.; Hari, Y.; Andoh, J.; Morio, K.; Doi, T.; Imanishi, T. *Tetrahedron Lett.* **1998**, *39*, 5401.
6. Singh, S. K.; Nielsen, P.; Koshkin, A. A.; Wengel, J. *Chem. Commun.* **1998**, *4*, 455.
7. Nielsen, K. E.; Singh, S. K.; Wengel, J.; Jacobsen, J. P. *Bioconjugate Chem.* **2000**, *11*, 228.

8. Bondensgaard, K.; Petersen, M.; Singh, S. K.; Rajwanshi, V. K.; Kumar, R.; Wengel, J.; Jacobsen, J. P. *Chem. Eur. J.* **2000**, *6*, 2687.
9. Braasch, D. A.; Corey, D. R. *Chem. Biol.* **2001**, *8*, 1.
10. Arzumanov, A.; Walsh, A. P.; Rajwanshi, V. K.; Kumar, R.; Wengel, J.; Gait, M. J. *Biochemistry* **2001**, *40*, 14645.
11. Vester, B.; Lundberg, L. B.; Sorensen, M. D.; Babu, B. R.; Douthwaite, S.; Wengel, J. *J. Am. Chem. Soc.* **2002**, *124*, 13682.
12. Randazzo, A.; Esposito, V.; Ohlenschlaeger, O.; Ramachandran, R.; Mayol, L. *Nucleosides Nucleotides Nucleic Acids* **2005**, *24*, 795–800.
13. Randazzo, A.; Esposito, V.; Ohlenschlaeger, O.; Ramachandran, R.; Virgilio, A.; Mayol, L. *Nucleic Acids Res.* **2004**, *32*, 3083.
14. Williamson, J. R.; Raghuraman, M. K.; Cech, T. R. *Cell* **1989**, *59*, 871.
15. Simonsson, T.; Pecinka, P.; Kubista, M. *Nucleic Acid Res.* **1998**, *26*, 1167.
16. Nimjee, S. M.; Rusconi, C. P.; Sullenger, B. A. *Annu. Rev. Med.* **2005**, *56*, 555.
17. Block, L. C.; Griffin, L. C.; Latham, J. A.; Vermaas, E. H.; Toole, J. J. *Nature* **1992**, *355*, 564.
18. Griffin, L. C.; Tidmarsh, G. F.; Bock, L. C.; Toole, J. J.; Leung, L. K. *Bloods* **1993**, *81*, 3271.
19. Li, W. X.; Kaplan, A. V.; Grant, G. W.; Toole, J. J.; Leung, L. L. *Blood* **1994**, *83*, 677.
20. Wang, K. Y.; McCurdy, S.; Shea, R. G.; Swaminathan, S.; Bolton, P. H. *Biochemistry* **1993**, *32*, 1899.
21. Macaya, R. F.; Schultze, P.; Smith, F. W.; Roe, J. A.; Feigon, J. *Proc. Natl. Acad. Sci. U.S.A.* **1993**, *90*, 3745.
22. Paborsky, L. R.; McCurdy, S. N.; Griffin, L. C.; Toole, J. J.; Leung, L. K. *J. Biol. Chem.* **1993**, *268*, 20808.
23. Dias, E.; Battiste, J. L.; Williamson, J. R. *J. Am. Chem. Soc.* **1994**, *116*, 4479.
24. He, G.-X.; Krawczyk, S. H.; Swaminathan, S.; Regan, S. G.; Dougherty, J. P.; Terhorst, T.; Law, V. S.; Griffin, L. C.; Coutrè, S.; Bischofberger, N. *J. Med. Chem.* **1998**, *41*, 2234.
25. He, G.-X.; Williams, J. P.; Postich, M. J.; Swaminathan, S.; Regan, S. G.; Terhorst, T.; Law, V. S.; Griffin, L. C.; Cheri, M. T.; Coutrè, S.; Bischofberger, N. *J. Med. Chem.* **1998**, *41*, 4224.
26. Smith, F. W.; Feigon, J. *Biochemistry* **1993**, *32*, 8682.
27. Wang, Y.; Patel, D. J. *Structure* **1993**, *1*, 263.
28. Lavery, R.; Sklenar, H. *J. Biomol. Struct. Dyn.* **1988**, *6*, 63.
29. Lavery, R.; Sklenar, H. *J. Biomol. Struct. Dyn.* **1989**, *6*, 655.
30. Lu, M.; Guo, Q.; Kallenbach, N. R. *Biochemistry* **1993**, *32*, 598.
31. Lu, M.; Guo, Q.; Kallenbach, N. R. *Biochemistry* **1993**, *32*, 3596.
32. Smirnov, I.; Shafer, R. H. *Biochemistry* **2000**, *39*, 1462.
33. Shafer, R. H. *Prog. Nucleic Acids Res. Mol. Biol.* **1998**, *59*, 55.
34. Petraccone, L.; Erra, E.; Nasti, L.; Galeone, A.; Randazzo, A.; Mayol, L.; Barone, G.; Giancola, C. *J. Biomol. Macromol.* **2002**, *31*, 131.
35. Padmanachan, K.; Tulinsky, A. *Acta Cryst.* **1996**, *D52*, 272.
36. Martino, L.; Virno, A.; Randazzo, A.; Virgilio, A.; Esposito, V.; Giancola, C.; Bucci, M.; Cirino, G.; Mayol, L. *Nucleic Acid Res.* **2006**, *34*, 6653.
37. Piotto, M.; Saudek, V.; Sklenar, V. J. *J. Biomol. NMR* **1992**, *2*, 661.
38. Jeener, J.; Meier, B.; Bachmann, H. P.; Ernst, R. R. *J. Chem. Phys.* **1979**, *71*, 4546.
39. Braunschweiler, L.; Ernst, R. R. *J. Magn. Reson.* **1983**, *53*, 521.
40. Marion, D.; Ikura, M.; Tschudin, R.; Bax, A. *J. Magn. Reson.* **1989**, *85*, 393.
41. Weiner, S. J.; Kollman, P. A.; Case, D. A.; Singh, U. C.; Ghio, C.; Alagona, G.; Profeta, S.; Weiner, P. J. *J. Am. Chem. Soc.* **1984**, *106*, 765.
42. Marky, L. A.; Breslauer, K. J. *Biopolymers* **1987**, *26*, 1601.